Designation: E1931 – 16

Standard Guide for Non-computed X-Ray Compton Scatter Tomography[1]

This standard is issued under the fixed designation E1931; the number immediately following the designation indicates the year of original adoption or, in the case of revision, the year of last revision. A number in parentheses indicates the year of last reapproval. A superscript epsilon (ε) indicates an editorial change since the last revision or reapproval.

1. Scope

1.1 *Purpose*—This guide covers a tutorial introduction to familiarize the reader with the operational capabilities and limitations inherent in a single non-computed X-ray Compton Scatter Tomography (CST). Also included is a brief description of the physics and typical hardware configuration for CST. This single technique is still used for a small number of inspections. This is not meant as comprehensive guide covering the variety of Compton scattering techniques that are now used for non-destructive testing and security screen screening.

1.2 *Advantages*—X-ray Compton Scatter Tomography (CST) is a radiologic nondestructive examination method with several advantages that include:

1.2.1 The ability to perform X-ray examination without access to the opposite side of the examination object;

1.2.2 The X-ray beam need not completely penetrate the examination object allowing thick objects to be partially examined. Thick examination objects become part of the radiation shielding thereby reducing the radiation hazard;

1.2.3 The ability to examine and image object subsurface features with minimal influence from surface features;

1.2.4 The ability to obtain high-contrast images from low subject contrast materials that normally produce low-contrast images when using traditional transmitted beam X-ray imaging methods; and

1.2.5 The ability to obtain depth information of object features thereby providing a three-dimensional examination. The ability to obtain depth information presupposes the use of a highly collimated detector system having a narrow angle of acceptance.

1.3 *Applications*—This guide does not specify which examination objects are suitable, or unsuitable, for CST. As with most nondestructive examination techniques, CST is highly application specific thereby requiring the suitability of the method to be first demonstrated in the application laboratory. This guide does not provide guidance in the standardized practice or application of CST techniques. No guidance is provided concerning the acceptance or rejection of examination objects examined with CST.

1.4 *Limitations*—As with all nondestructive examination methods, CST has limitations and is complementary to other NDE methods. Chief among the limitations is the difficulty in performing CST on thick sections of high-*Z* materials. CST is best applied to thinner sections of lower *Z* materials. The following provides a general idea of the range of CST applicability when using a 160 keV constant potential X-ray source:

Material	Practical Thickness Range
Steel	Up to about 3 mm (⅛ in.)
Aluminum	Up to about 25 mm (1 in.)
Aerospace composites	Up to about 50 mm (2 in.)
Polyurethane Foam	Up to about 300 mm (12 in.)

The limitations of the technique must also consider the required *X*, *Y*, and *Z* axis resolutions, the speed of image formation, image quality and the difference in the X-ray scattering characteristics of the parent material and the internal features that are to be imaged.

1.5 The values stated in both inch-pound and SI units are to be regarded separately as the standard. The values given in parentheses are for information only.

1.6 *This standard does not purport to address all of the safety concerns, if any, associated with its use. It is the responsibility of the user of this standard to establish appropriate safety and health practices and to determine the applicability of regulatory limitations prior to use.*

2. Referenced Documents

2.1 *ASTM Standards:*[2]

E747 Practice for Design, Manufacture and Material Grouping Classification of Wire Image Quality Indicators (IQI) Used for Radiology

E1025 Practice for Design, Manufacture, and Material Grouping Classification of Hole-Type Image Quality Indicators (IQI) Used for Radiology

E1255 Practice for Radioscopy

[1] This guide is under the jurisdiction of ASTM Committee E07 on Nondestructive Testing and is the direct responsibility of E07.01 on Radiology (X and Gamma) Method.

Current edition approved June 1, 2016. Published June 2016. Originally approved in 1997. Last previous edition approved in 2009 as E1931 – 09. DOI: 10.1520/E1931-16.

[2] For referenced ASTM standards, visit the ASTM website, www.astm.org, or contact ASTM Customer Service at service@astm.org. For *Annual Book of ASTM Standards* volume information, refer to the standard's Document Summary page on the ASTM website.

E1316 Terminology for Nondestructive Examinations
E1441 Guide for Computed Tomography (CT) Imaging
E1453 Guide for Storage of Magnetic Tape Media that Contains Analog or Digital Radioscopic Data
E1475 Guide for Data Fields for Computerized Transfer of Digital Radiological Examination Data
E1647 Practice for Determining Contrast Sensitivity in Radiology

2.2 *ANSI/ASNT Standards:*[3]

SNT-TC-1A ASNT Recommended Practice for Personnel Qualification and Certification in Nondestructive Testing
ANSI/ASNT CP-189 Standard for Qualification and Certification in Nondestructive Testing Personnel

2.3 *Military Standard*:

MIL-STD-410 Nondestructive Testing Personnel Qualification and Certification[4]

2.4 *Aerospace Standard:*[5]

AIA-NAS-410 Aerospace Industries Association, National Aerospace Standard-4105 Certification and Qualification of Nondestructive Test Personnel[6]

2.5 *ISO Standard:*[7]

ISO 9712 Nondestructive Testing—Qualification and Certification of NDT Personnel

3. Terminology

3.1 *Definitions:*

3.1.1 CST, being a radiologic examination method, uses much the same vocabulary as other X-ray examination methods. A number of terms used in this standard are defined in Terminology E1316. It may also be helpful to read Guide E1441.

4. Summary of Guide

4.1 *Description*—Compton Scatter Tomography is a uniquely different nondestructive test method utilizing penetrating X-ray or gamma-ray radiation. Unlike computed tomography (CT), CST produces radioscopic images which are not computed images. Multiple slice images can be simultaneously produced so that the time per slice image is in the range of a few seconds. CST can produce images that are thin with respect to the examination object thickness (slice images) and which are at right angles to the X-ray beam. Each two-dimensional slice image (*X*–*Y* axes) is produced at an incremental distance along and orthogonal to the X-ray beam (*Z*–axis). A stack of CST images therefore represents a solid volume within the examination object. Each slice image contains examination object information which lies predominantly within the desired slice. To make an analogy as to how CST works, consider a book. The examination object may be larger or smaller (in length, width and depth) then the analogous book. The CST slice images are the pages in the book. Paging through the slice images provides information about examination object features lying at different depths within the examination object.

4.2 *Image Formation*—CST produces one or more digital slice plane images per scan. Multiple slice images can be produced in times ranging from a few seconds to a few minutes depending upon the examined area, desired spatial resolution and signal-to-noise ratio. The image is digital and is typically assembled by computer. CST images are free from reconstruction artifacts as the CST image is produced directly and is not a calculated image. Because CST images are digital, they may be enhanced, analyzed, archived and in general handled as any other digital information.

4.3 *Calibration Standards*—As with all nondestructive examinations, known standards are required for the calibration and performance monitoring of the CST method. Practice E1255 calibration block standards that are representative of the actual examination object are the best means for CST performance monitoring. Conventional radiologic performance measuring devices, such as Test Method E747 and Practice E1025 image quality indicators or Practice E1647 contrast sensitivity gages are designed for transmitted X-ray beam imaging and are of little use for CST. With appropriate calibration, CST can be utilized to make three-dimensional measurements of internal examination object features.

5. Significance and Use

5.1 *Principal Advantage of Compton Scatter Tomography*—The principal advantage of CST is the ability to perform three-dimensional X-ray examination without the requirement for access to the back side of the examination object. CST offers the possibility to perform X-ray examination that is not possible by any other method. The CST sub-surface slice image is minimally affected by examination object features outside the plane of examination. The result is a radioscopic image that contains information primarily from the slice plane. Scattered radiation limits image quality in normal radiographic and radioscopic imaging. Scatter radiation does not have the same detrimental effect upon CST because scatter radiation is used to form the image. In fact, the more radiation the examination object scatters, the better the CST result. Low subject contrast materials that cannot be imaged well by conventional radiographic and radioscopic means are often excellent candidates for CST. Very high contrast sensitivities and excellent spatial resolution are possible with CST tomography.

5.2 *Limitations*—As with any nondestructive testing method, CST has its limitations. The technique is useful on reasonably thick sections of low-density materials. While a 25 mm (1 in.) depth in aluminum or 50 mm (2 in.) in plastic is achievable, the examination depth is decreased dramatically as the material density increases. Proper image interpretation requires the use of standards and examination objects with

[3] Available from American National Standards Institute (ANSI), 25 W. 43rd St., 4th Floor, New York, NY 10036, http://www.ansi.org.
[4] Available from Standardization Documents Order Desk, DODSSP, Bldg. 4, Section D, 700 Robbins Ave., Philadelphia, PA 19111-5098, http://www.dodssp.daps.mil.
[5] Available from Federal Aviation Administration (FAA), 800 Independence Ave., SW, Washington, DC 20591, http://www.faa.gov.
[6] This document has superseded MIL-STD-410; however, MIL-STD-410 is still acceptable to the FAA
[7] Available from International Organization for Standardization (ISO), ISO Central Secretariat, BIBC II, Chemin de Blandonnet 8, CP 401, 1214 Vernier, Geneva, Switzerland, http://www.iso.org.

known internal conditions or representative quality indicators (RQIs). The examination volume is typically small, on the order of a few cubic inches and may require a few minutes to image. Therefore, completely examining large structures with CST requires intensive re-positioning of the examination volume that can be time-consuming. As with other penetrating radiation methods, the radiation hazard must be properly addressed.

6. Basis of Application

6.1 Personnel Qualification is subject to contractual agreement between the parties using or referencing this standard.

6.1.1 If specified in the contractual agreement, personnel performing examinations to this standard shall be qualified in accordance with a nationally or internationally recognized NDT personnel qualification practice or standard such as ANSI/ASNT-CP-189, SNT-TC-1A, NAS-410, MIL-STD-410E, ISO 9712, or a similar document and certified by the employer or certifying agency, as applicable. The practice or standard used and its applicable revision shall be identified in the contractual agreement between the using parties.

7. Technical Description

7.1 *General Description of Compton Scatter Tomography*—Transmitted beam radiologic techniques used in radiography, radioscopy and computed tomography have dominated the use of penetrating radiation for industrial nondestructive examination. The transmitted beam technique depends upon the penetrating radiation attenuation mechanisms of photoelectric absorption and Compton scattering. For low- Z materials at energies up to about 50 keV, the photoelectric effect is the dominant attenuation mechanism. As X-ray energy increases, Compton scattering becomes the dominant attenuation mechanism. Pair production comes into play above 1.02 MeV and can become the dominant effect for higher X-ray energies. The following relationships are plotted in Fig. 1 and show the approximate dependence of the photoelectric effect and Compton scattering upon target material atomic number (Z) and incident X-ray energy (E):

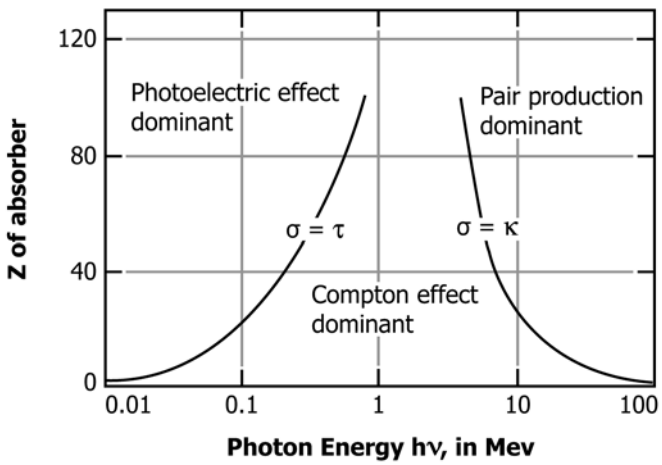

FIG. 1 Relationship Between Photoelectric, Compton, and Pair Production Effects

Photoelectric Effect: $\tau = Z^{5} / E^{7/2}$
Compton Scattering: $\sigma = Z / E$
Pair Production : $\kappa = Z^{2}$ ($ln\ E$ - constant)

The terms τ, σ, and κ represent the cross sections of the photoelectric, Compton scatter and pair-production interaction of a given X-ray photon that has energy level E. There is no analytic expression for the probability of photoelectric absorption as it varies as a function of E and Z. For the gamma and X-ray energies of interest, the exponent of Z can vary between 4 and 5.[8] The green lines are contours where the indicated cross sections are equal. Since the cross sections are proportional to the probability of the particular type of interaction, moving left to right in the graph, the green lines represent the boundaries of the regions where the photoelectric, Compton and pair-production events are dominant, respectively. The graph is useful for understanding the X-ray properties of a material, by knowing its predominant mass number Z. For example, it could be used to estimate its interaction regime based on the Z of the material and energy of interrogation photons.

7.1.1 CST is best suited for lower Z materials such as aluminum (Z=13) using a commercially available 160 keV X-ray generating system. Somewhat higher Z materials may be examined by utilizing a higher energy X-ray generator rated at 225, 320, or 450 keV.

7.1.2 It is useful to envision the CST process as one where the X-rays that produce the CST image originate from many discrete points within the examined volume. Each Compton scatter event generates a lower energy X ray that emanates from the scattering site. Singly scattered X rays that reach the detector carry information about the examination object material characteristics at the site where it was generated. The scatter radiation is also affected by the material through which it passes on the way to the detector. The external source of primary penetrating radiation, that may be either X rays or gamma rays, interact by the Compton scattering process. The primary radiation must have adequate energy and intensity to generate sufficient scattered radiation at the examination site to allow detection. The examination depth is limited to that depth from which sufficient scattered radiation can reach the detector to form a usable image. The examination object is therefore effectively imaged from the inside out. The CST image is formed voxel (volume element) by voxel in raster fashion where the detector's field-of-view intersects with the central X-ray beam at the examination site. The primary radiation beam source and scattered radiation detector are highly collimated to assure collection of single-scattered radiation from a known small volume of the examination object. Multiple scattered radiation causes a loss of spatial resolution, but can enhance contrast of features. Moving the intersection of the radiation source and detector lines of sight in a systematic fashion allows a tomogram, or slice image to be produced. Changing the distance at which the radiation source and detector lines of sight intersect allows the tomogram to be produced at a selected depth below the examination object surface.

[8] Knoll, G. F., *Radiation Detection and Measurement*, 3rd Ed. John Wiley and Sons, New York, 2000.

7.2 *Significant Differences in the Transmitted Beam and Compton Scattered X-Ray Imaging Techniques*—The differences between conventional transmitted beam and Compton Scatter Imaging are so significant that CST must be considered a separate examination technique. For transmitted beam techniques, the radiation source characteristics must be carefully controlled. The energy and intensity must be selected carefully to fully penetrate the object and provide the required contrast sensitivity. Thick sections of high-density materials require a high-energy radiation source while thin sections of low-density materials require a low-energy radiation source. For CST applications, the energy and intensity of the primary radiation beam is relatively less important. The primary radiation beam energy and intensity are not critical as long as they remain stable and are sufficient to generate adequate scatter radiation at the CST examination depth. Small focal spot size is critical to transmitted beam image sharpness. The primary radiation focal spot size is also of significant importance for CST. For CST the beam must be collimated. A smaller focal spot can have a shorter collimator to achieve the same level of collimation. The $1/R^2$ (where R is the distance from the object) effect for X-ray source allows a high power, small focal spot X-ray tube (1.0 mm X-ray focal spot size (FOC) at 1800 W), to have a higher flux than a standard X-ray tube (5.5 mm FOC at 3000W) while maintaining the same image quality. For this reason an X-ray source is often a better choice than a radioisotope for CST. Radiation detection and other image forming considerations may also differ substantially from other radiologic imaging methods.

7.3 *Theory of Compton Scatter Tomography*—In the energy range appropriate for CST (roughly 50 keV to 1 MeV), the primary interaction mechanisms between electromagnetic radiation and matter are photoelectric absorption and inelastic (Compton) scatter. Fig. 2 illustrates the principles of photoelectric absorption and Compton scattering. As an X ray having an energy E_0 collides with an electron, the electron absorbs energy from the incoming X-ray photon and is ejected from its shell. In the case of photoelectric absorption, the incoming photon's energy is totally absorbed. As the energy E_0 of the incoming photon increases, the probability of photoelectric absorption decreases while the probability of Compton scattering increases. The Compton scattering creates a new X ray having and energy E', and travelling at an angle θ with respect to the direction of the original primary X ray.

7.3.1 Material linear attenuation coefficients due to photoelectric absorption and Compton scattering vary with energy. The linear absorption coefficient μ_τ falls sharply with increasing energy, while the scatter coefficient μ_σ remains nearly constant. For low-*Z* materials, scatter begins to dominate photoelectric absorption at primary radiation energies above 50 keV allowing the use of scatter radiation instead of the attenuated primary beam radiation for imaging purposes. It should also be noted that unlike the linear attenuation coefficient, the scatter coefficient is relatively independent of the primary penetrating radiation energy E_0. Many of the restrictions on energy selection associated with transmitted beam techniques are not a consideration with CST. For example, low-density aerospace composite materials can be

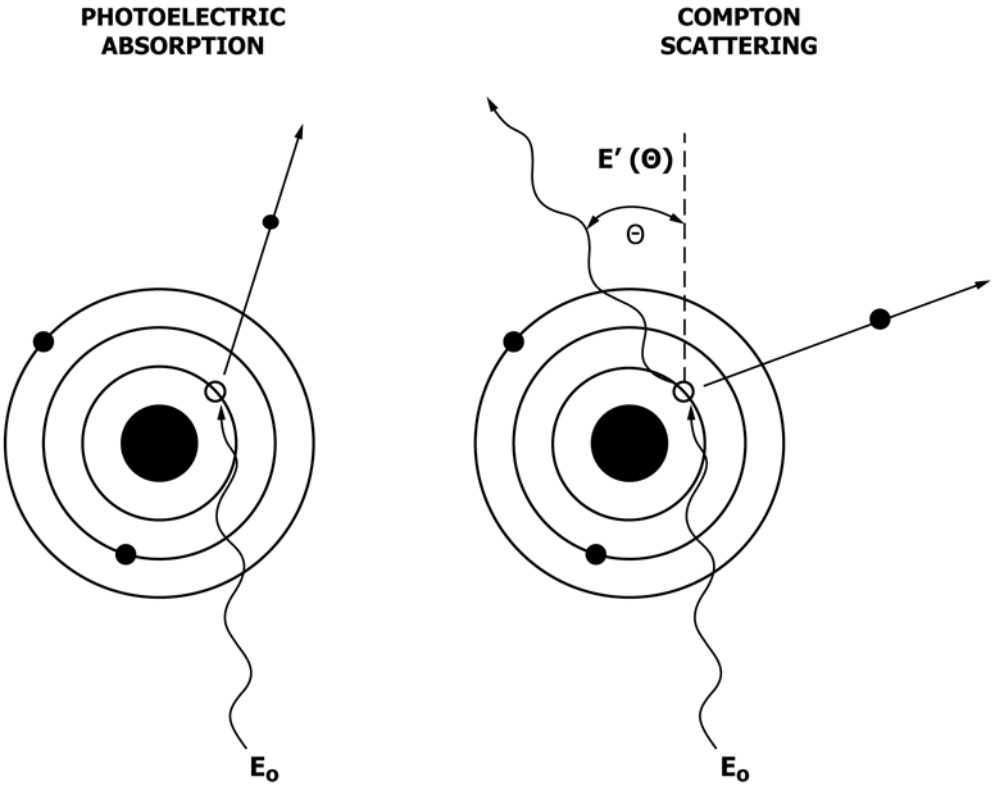

FIG. 2 Principles of Photoelectric Absorption and Compton Scattering

imaged at higher energies of 100 keV or more producing high contrast using CST techniques.

7.3.2 The energy of the scattered X ray is given by:

$$E' = \frac{E_0}{1+\left(\frac{E_0}{m_e c^2}\right)(1 - \cos\theta)} \quad (1)$$

where:

E' = energy of the scattered X ray,
E_0 = energy of the primary radiation photon,
c = speed of light,
$m_e c^2$ = rest energy of the electron,
m_e = electron mass, and
θ = scattering angle.

It can be seen from Eq 1 that the energy of the scatter radiation E' decreases with increasing scattering angle θ. The amount of Compton scattering in any material is proportional to its electron density.

7.3.3 Disregarding the effects of pair production that come into play above 1.02 MeV, the total attenuation is the sum of attenuation due to photoelectric absorption and Compton scattering:

$$\mu = \mu_\tau + \mu_\sigma \quad (2)$$

where μ, μ_τ, and μ_σ are the total, photoelectric-absorption and Compton scattering linear attenuation coefficients, respectively.

Fig. 3 is a polar plot of the Klein Nishina Compton scatter (free electron scattering) angular intensity at 30 and 300 keV. Although the scatter radiation angular distribution becomes more intense in the forward direction as energy increases, there is sufficient intensity at all angles to permit the technique. The detector and the primary radiation source can therefore be positioned on the same side of the examination object in this energy range.

7.3.4 The intensity of radiation I_{SC} scattered from a volume element (voxel) V_{Voxel} inside the examination object can be approximated as follows:

$$I_{SC} = K \cdot n_e \cdot V_{Voxel} \cdot I_0 e^{-\mu\tau}\left(1 - e^{-\mu_c W}\right)\left(e^{-\mu' t'}\right) + M \quad (3)$$

where:

K = constant of proportionality representing the differential scatter cross-section, detector efficiencies and all other object-dependent effects,
n_e = number of electrons per unit volume acting as scatter centers,
I_0 = incident flux,
$e^{-\mu t}$ = the attenuation along the primary beam path,
$1-e^{-\mu\sigma W}$ = the fraction of photons scattered from the primary beam in a voxel of length W. The scattering voxel is the intersection of the incident pencil beam with the solid angle subtended by the detector,
dV = the volume of the scattering voxel,
W = length of the scattering voxel along the path of the pencil beam,
$\mu\sigma$ = the Compton linear attenuation coefficient, as defined earlier,
$e^{-\mu' t'}$ = the attenuation along the scattered beam path t'. μ' is the total linear attenuation coefficient of the lower energy scattered beam,
μ' = the total linear attenuation coefficient of the lower energy scattered beam, and
M = multiple scatter component originating from quanta scattered more than once outside the voxel.

The two exponential terms describe the radiation attenuation along the primary radiation beam path t as well as the scattered beam path t'. Due to the lower X-ray energy along the scatter path, μ' is not equal to μ. The last term represents the contribution of photons that are scattered from other voxels, scattered more than once, and scattered into the solid angle of the pixel. The influence of this type of multiple scatter radiation needs to be minimized because it degrades the fidelity of image information corresponding to the voxel of interest, where the primary scatter originated. This may be accomplished by tightly collimating the detector to limit its field-of-view to the desired examination voxel and by software.

7.4 *Contrast Sensitivity*—One significant benefit of CST as compared with conventional transmission imaging is increased

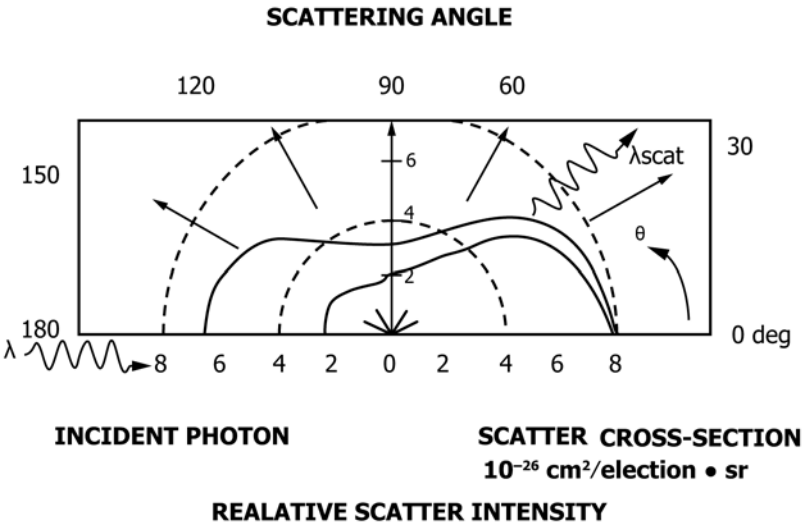

FIG. 3 Polar Plot of Relative Scatter Intensity as a Function of Scattering Angle at Primary Radiation Energies of 30 and 300 keV

contrast sensitivity. Fig. 4 is a generalized representation of transmission beam imaging to determine the relationship between discontinuity size and subject contrast.

7.4.1 To find an expression for the sensitivity of the transmitted beam technique, consider a homogeneous material of thickness L whose attenuation coefficient is μ except for a small discontinuity region of length W and whose attenuation coefficient is μ_D.

7.4.1.1 The intensities of the radiation beams passing through the homogeneous examination object with and without the small discontinuity are I_T and $I_{T'}$, respectively, given by:

$$I_T = I_0 e^{-\mu L} \tag{4}$$

$$I_{T'} = I_0 e^{-(\mu(L - W) + \mu_D W)} \tag{5}$$

From these equations the subject contrast C is expressed as follows:

$$C = \frac{(I_{T'} - I_T)}{I_T} \times 100\,\% \tag{6}$$

$$C = \frac{e^{(-\mu(L - W)L + \mu_D W)} - e^{-\mu L}}{e^{-\mu L}} \tag{7}$$

Assuming a small discontinuity allows the exponent to be replaced by its power expansion to the first order providing the following expression:

$$C = e^{-(\mu_D - \mu)W} - 1 \tag{8}$$

$$C = (1 - (\mu_D - \mu)W) - 1 = (\mu - \mu_D)W \tag{9}$$

Thus, in a transmission imaging system, contrast is directly proportional to the discontinuity size.

7.4.2 Fig. 5 is a generalized representation of a CST system. The examination object of thickness *L* contains a small discontinuity of length *W* and having a linear attenuation coefficient of μ_D.

7.4.2.1 The CST system contrast may be determined by comparing the scatter signals, I_{SC} and $I_{SC'}$, from two similarly located voxels. For one sided radiographic inspection using backscatter imaging, the scatter signal is:[9]

$$I_{SC} = I_0 e^{-\mu_1 x_1} \mu_{scat} W e^{-\mu_2 x_2} \tag{10}$$

with μ_1 and μ_2 being the total attenuation coefficients for the entering and the scattered beam, x_1 and x_2 being the path lengths of entering and scattered beam in the base material, $\mu_{scat}W$ the probability of scatter in the scatter voxel by a material with linear scatter coefficient μ_{scat} and a thickness *W*. If the material in the scatter voxel at the same location changes to $\mu_{D,scat}$ the scatter signal becomes:

$$I_{sc}' = I_0 e^{-\mu_1 x_1} \mu_{D,scat} W e^{-\mu_2 x_2} \tag{11}$$

The total attenuation coefficient for the scattered beam does not change because the energy shift depends only on the scatter angle but not on the photon energy (see Eq 1). Accordingly, the contrast is:

$$C = \frac{I_{sc} - I_{sc'}}{I_{sc}} = \frac{I_0 e^{-\mu_1 x_1} \mu_{scat} W e^{-\mu_2 x_2} - I_0 e^{-\mu_1 x_1} \mu_{D,scat} W e^{-\mu_2 x_2}}{I_0 e^{-\mu_1 x_1} \mu_{scat} W e^{-\mu_{12} x_2}}$$

$$= \frac{\mu_{scat} - \mu_{D,scat}}{\mu_{scat}} \tag{12}$$

Again, here μ_{scat} and $\mu_{D,scat}$ are the linear scatter coefficients in the scatter voxel.

7.4.3 CST contrast depends upon the ratio of the scattering coefficients of the parent material (μ) and the discontinuity (μ_D) and is independent of the object thickness. Assuming an air-filled discontinuity (no scatter) in aluminum with an examination voxel lying wholly within the discontinuity, scatter

[9] Bossi, R. H., Friddell, K. D., Nelson, J. M. "Backscatter X-Ray Imaging," *Mat. Eval., 46*, 1988, pp. 1462–67.

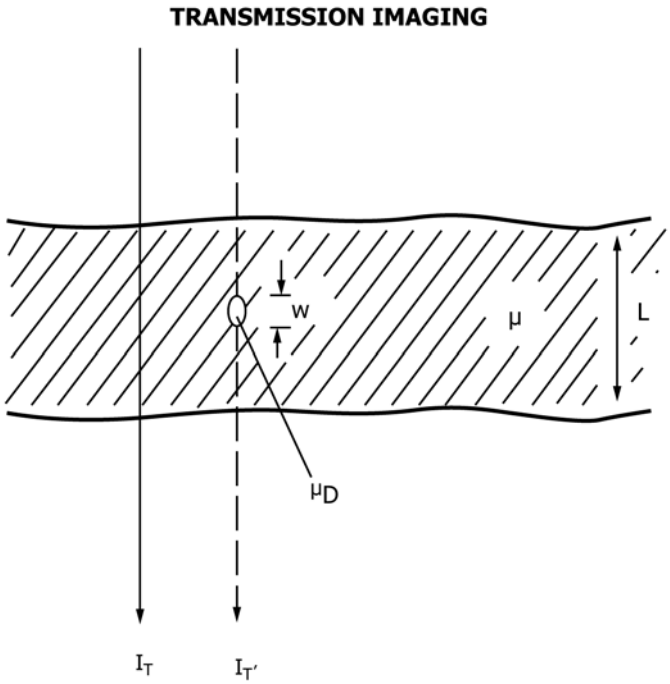

FIG. 4 Schematic Representation of the Transmitted Beam Imaging System Technique

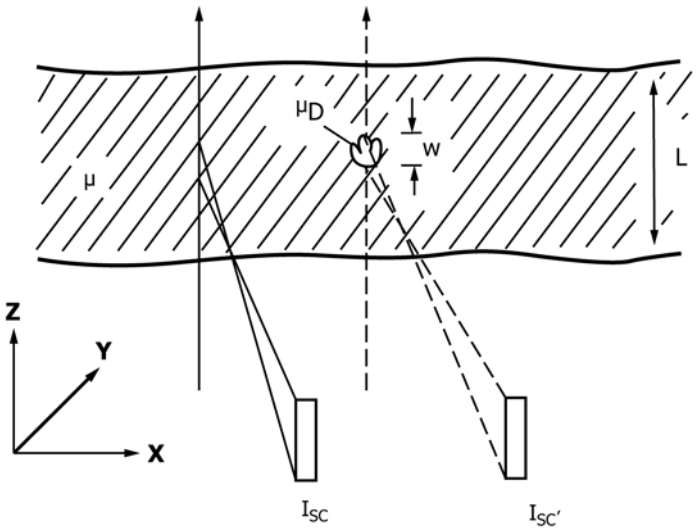

FIG. 5 Schematic Representation of the Compton Scatter Tomography Technique

imaging contrast approaches 100 % for a small void. However, even a high-contrast CST image can be lost to noise if the technique is improperly applied.

7.4.4 An important consideration for CST is that the material between the scattering voxels in the region of interest and the detector must not unduly attenuate the scattered radiation or the CST signal can become so weak it is lost in the noise. Therefore, the most successful implementations of CST are those involving relatively thin sections of low-density materials where the region of interest lies relatively close to the surface.

7.5 *Sensitivity Compared to Transmission Imaging*—Transmission imaging contrast sensitivity depends upon the often very small difference between the radiation intensities of the parent material path and the parent material with discontinuity path. On the other hand, scatter imaging contrast depends upon the often large difference between the scattering coefficients of the parent material and the discontinuity. If the discontinuity is a void, it may scatter little, if any, radiation while the parent material scatters considerably thus yielding useful contrast.

7.5.1 The contrast sensitivity offered by CST can be much higher than for transmission imaging as long as the difference in the parent material and discontinuity signal is greater than the statistical fluctuations due to system and radiation noise. The higher contrast of the CST method is of practical value only if the noise levels are the same in both methods. Therefore, the contrast/noise ratio is of value for a comparison of CST and transmission imaging systems. Noise factors for transmission and CST systems, respectively, may be represented as follows:

$$\sqrt{\frac{1}{N_{trans}}} \tag{13}$$

and:

$$\sqrt{\frac{1}{N_{scat}}} \tag{14}$$

where N_{trans} and N_{scat} represent the nominal number of photons detected by the pixel element and is proportional to the exposure level, which in turn is affected by the exposure time, flux or X-ray tube filament current. These two expressions follow from considering the noise factor to be the noise to signal level, and assuming Poisson statistics. The signal power (signal level squared) divided by the noise power (i.e., the variance of the noise) is proportional to the number of photons, so the noise-to-signal level is the square root of the reciprocal of this quantity.

7.5.2 Defining the sensitivity of both CST and transmission imaging as the difference in signals in an examination object having a thickness equal to L with and without a small discontinuity at a depth L divided by the noise factor it follows:

$$S_{trans} = (\mu - \mu_D) W \sqrt{N_{trans}} \tag{15}$$

$$S_{scat} = \frac{\mu_{scat} - \mu_{D,scat}}{\mu_{scat}} \sqrt{N_{scat}} = 1 - \frac{\mu_{D,scat}}{\mu_{scat}} \sqrt{N_{scat}} \tag{16}$$

where S_{trans} and S_{scat} are the sensitivity of the transmission and CST systems, respectively.

7.6 *In-Plane Spatial Resolution*—Spatial resolution for CST can compare favorably with the radioscopic transmission imaging technique. However, it must be remembered that spatial resolution for the CST technique is a three-dimensional (X, Y, Z) figure of merit while only two-dimensional (X, Y) for the transmission imaging system. It is nevertheless useful to compare the sensitivity of small in-plane features for the CST technique with conventional transmission imaging system performance. It can be seen from Fig. 5 that the CST image voxel is formed by the intersection of the primary radiation beam and the detector fields-of-view. This volume determines the smallest geometric feature which can be imaged. Spatial

resolution for the CST technique is therefore determined by the dimensions of the primary radiation beam and the detector fields-of-view at the voxel and is a function of the angle between the primary central radiation beam and the detector's line-of-sight. Collimation of both the primary radiation beam and detector and the angle between the central primary radiation beam and the detector's line-of-sight may be selected to determine the required in-plane *X- Y* spatial resolution. However, the smaller the X-ray beam and the detector field-of-view become, the slower the examination speed. This is due to fewer Compton scattered X rays being produced per unit time and fewer singly-scattered Compton X rays being detected per unit time. Therefore, there is a trade-off between spatial resolution and examination speed. In-plane *X-Y* spatial resolution may be well within the submillimetre range.

7.7 *Tomographic Slice Thickness*— Tomographic slice thickness, or *Z*-axis resolution, is also a function of the primary radiation beam and detector collimation and the angle between the central primary radiation beam and the detector's line-of sight. Tomographic slice thickness can be well within the submillimetre range.

7.8 *Selection of the Tomographic Plane*—It may also be seen from Fig. 5 that the plane of examination is determined by where the central primary radiation beam and the detector's line-of-sight intersect along the *Z*-axis. The plane of examination may be selected by changing the primary radiation source and detector distance to the examination object or by adjusting the angle between the central radiation beam and the detector's line-of-sight.

7.9 *Examination Speed*—Examination speed is highly dependent upon a number of factors including the radiation source and collimation, the detector and collimation, the selected spatial resolution, allowable noise, material density, tomographic slice depth in the material and scan plan parameters. Fig. 6 shows a typical scan plan where the radiation source and detector (not shown) are moved with respect to the examination object in the *X-Y* plane. In the example shown, 250 data points are collected along the direction of travel with 500 scan line index steps. For example, this scan plan might cover a 25 by 50 mm (1 by 2 in.) area and require from 1 to 6 min to collect the data. Larger areas are examined by repositioning the radiation source and detector with respect to the

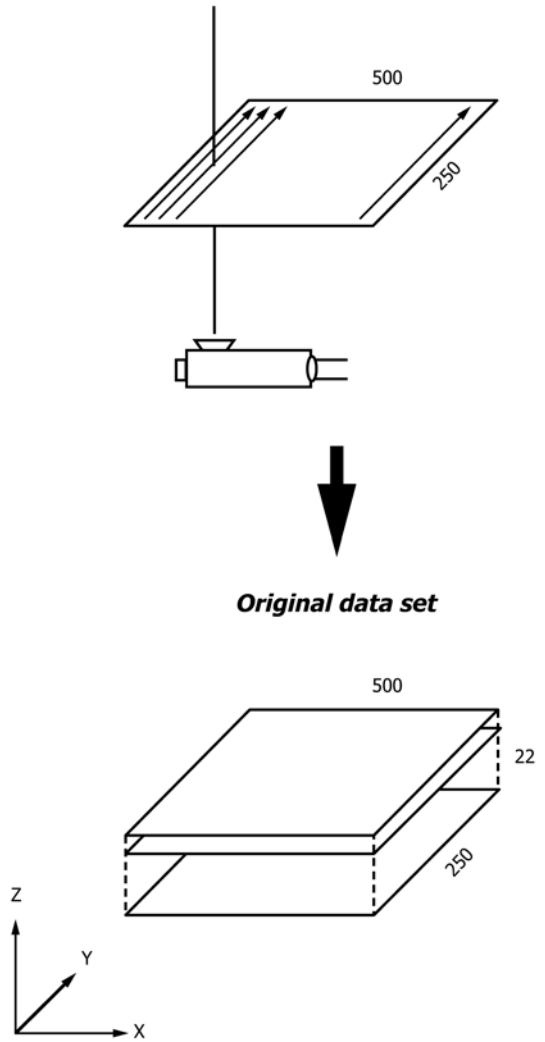

FIG. 6 Typical CST Imaging Scan Plan

examination object and repeating the raster scan. It is possible to perform simultaneous examination of multiple tomographic slices at increasing depths to speed the examination process. This may be accomplished by the use of multiple detectors arranged at slightly different angles with respect to the central radiation beam. Scattering is produced from a range of depths as the primary radiation beam passes the examination object. Tomographic-plane examination depth is set by the intersection of the central primary radiation beam with the detector's line-of-sight. In the example shown in Fig. 6, tomographic data is simultaneously collected from twenty-two imaging planes. The examination object material thickness represented by the twenty-two planes is a function of slice image plane thickness and plane-to-plane spacing.

7.10 *Examination Object Size Limitations*—One of the real advantages of CST is that there is no examination object size limitation (*X, Y*). This is due to the fact that the radiation source and detector are on the same side and may be positioned anywhere there is physical access to the region of examination object interest. Since there is not a requirement for the primary radiation beam to completely penetrate the examination object, the examination object can be thick with respect to the beam's penetrating power. The examination depth is limited primarily by the ability of sufficient numbers of low-energy Compton X rays to reach the detector with sufficient energy to be detected. There is no requirement for direct access to the examination part surface since the CST technique is non-contact. Stand-off distances in the range of several centimetres are practical. It should be remembered that while there are no examination object size limitations, there are limitations as to the examination depth (*Z*). The examination depth must be radioscopically thin where $\mu L < 1$. With a 160 keV X-ray source, examination depths of several centimetres are possible in aluminum. With less dense materials, such as aerospace composites, the examination depth may increase to tens of centimetres. In steel the examination depth may be in the range of millimetres. Increasing the primary radiation beam energy will increase the examination depth.

7.11 *CST Image Formation*—The CST image is formed in computer memory as a three-dimensional representation of voxel *X-Y* position versus detected scattered X-ray intensity. As the scanning process shown in Fig. 6 progresses, the encoded *X- Y* positions are fed to a computer. Simultaneously, the detected radiation intensity is fed to the computer and a three-dimensional map of *X* position, *Y* position and brightness (radiation intensity) is formed for each depth, *Z*. The image display is similar to a normal radioscopic image display. However, only information contained within a defined plane is presented. Image data from several tomographic planes may be simultaneously processed by multiplexing the input data. Fig. 7 is a simulated CST image display of a homogeneous examination object containing a spherical void. The void extends from a depth beginning at Plane 2 to a depth represented by Plane 6. The void produces no scatter radiation with respect to the parent material which produces scatter.

7.12 *Artifacts*—CST has no computational artifacts as the CST image is produced directly from raw scattered X-ray data. However, CST, like any imaging process has artifacts which are unique to CST.

7.12.1 Features lying outside the slice thickness can affect the scattered X-ray photon on its way to the detector thereby altering the scattered radiation signal. This can give the appearance of a lower density feature than actually lies in the image slice. Additional (multiple) scatter of the original scattered X ray caused by either the homogeneous bulk material or an anomaly (high- or low-density inclusion) in the detector's line of sight can cause artifacts in the CST image. Very tight detector collimation as well as software corrections can minimize the effect of multiple scatter. A high-or low-density inclusion in the detector's line of sight can also change the effective total absorption along the scattered photon's trajectory, thereby causing an image artifact. Slightly repositioning the CST setup with respect to the examination object can often determine whether an indicated feature lies in the desired slice plane or is an anomaly. If the suspected low-density feature remains stationary with respect to other slice features when the setup is re-positioned, it is a valid indication. If the suspected low-density feature moves with respect to other slice features, it does not lie in the desired slice. Multiple scans over an area is the penalty for improved interpretation.

8. Apparatus

8.1 Like modern radioscopic systems, CST systems comprise a number of subsystems (see Fig. 8) that generally include:

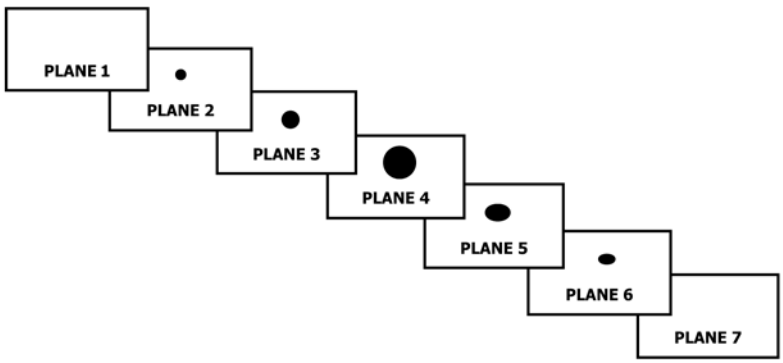

FIG. 7 Simulated CST Image Display of a Homogenous Examination Object Containing a Void

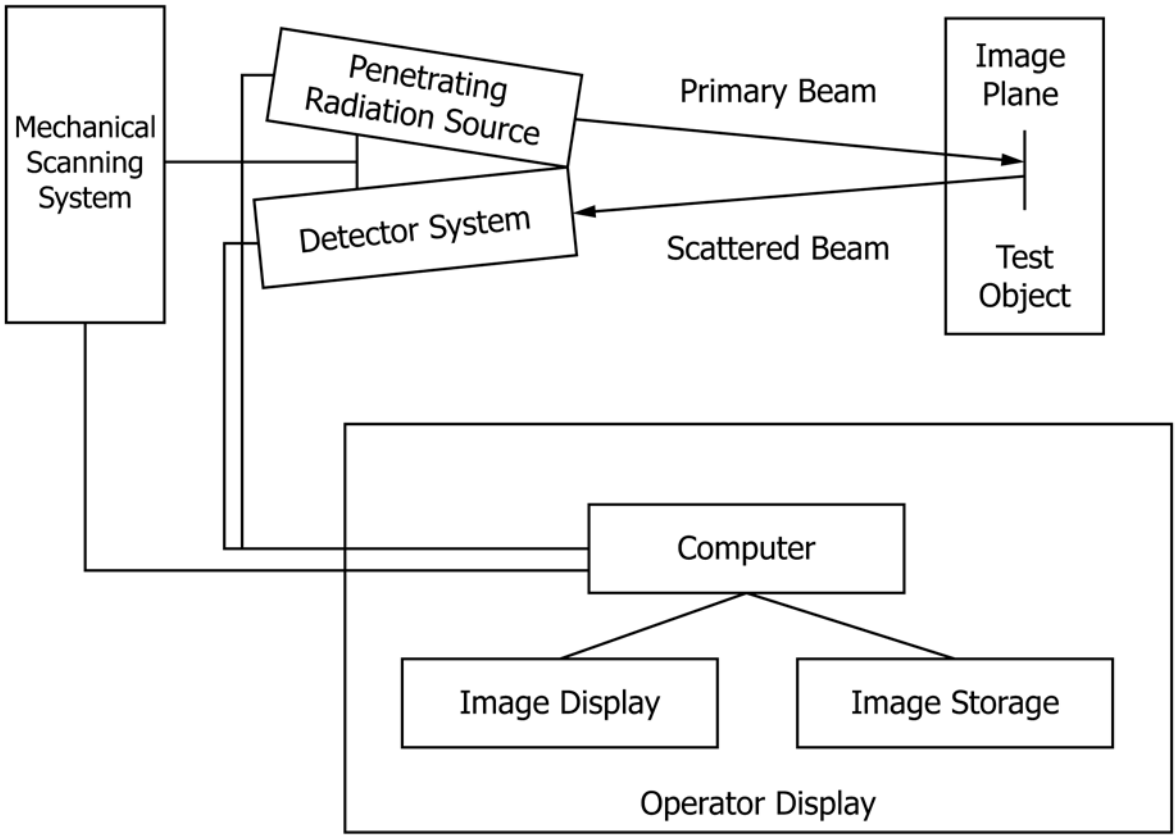

FIG. 8 Typical CST System Block Diagram

8.1.1 A source of penetrating radiation,
8.1.2 A radiation detector, or array of detectors,
8.1.3 A mechanical scanning system,
8.1.4 A computer system,
8.1.5 An image display system,
8.1.6 An image data storage system, and
8.1.7 An operator interface.

8.2 *Radiation Sources*—X-ray as well as gamma-ray sources have been successfully used for CST. Since the primary radiation source serves only to excite the Compton scattering process, the radiation source should be optimized for this process. From an energy standpoint, the radiation source must be sufficiently energetic to penetrate the examination object material to at least the required depth and excite the Compton scattering process. The resulting Compton scattered X rays must be sufficiently energetic to exit the examination object and reach the detector. However, the radiation source should not be excessively energetic for two reasons: the probability of an interaction with an electron decreases with increasing energy; and the difficulty of completely shielding the nearby detector from radiation source crosstalk increases. Therefore, the primary radiation energy must be appropriately selected. Another important consideration is radiation intensity, or the number of photons per unit time delivered to the examination voxel. In terms of energy selection, radiation beam intensity, and safety, the X-ray source is preferred over the radioisotope.

8.3 *Detectors*—The selection of a detector for Compton scattered X rays is very important to the success of the CST system. Because the scattered radiation intensity is very low, the detector will most likely be operated in a counting mode. The detector must exhibit excellent conversion efficiency and a fast recovery time. The scattered radiation energy is often very low so that the detector must exhibit low inherent filtration, high sensitivity and low noise. If the CST imaging system is to involve multiple detectors in a compact design, the detectors must also be small. Three classes of detectors which can be successfully used for CST are scintillation, ionization and solid state detectors.

8.4 *General CST Arrangement*—There are many possible arrangements for the radiation source and detector for CST. One such general arrangement is shown in Fig. 9 and uses nine detectors, for example. In this arrangement, the conical X-ray beam is collimated to form a small-diameter pencil beam. By action of a small aperture that is common to all detectors, each of the nine detectors receives scattered radiation originating from selected depths in the examination object. Each detector

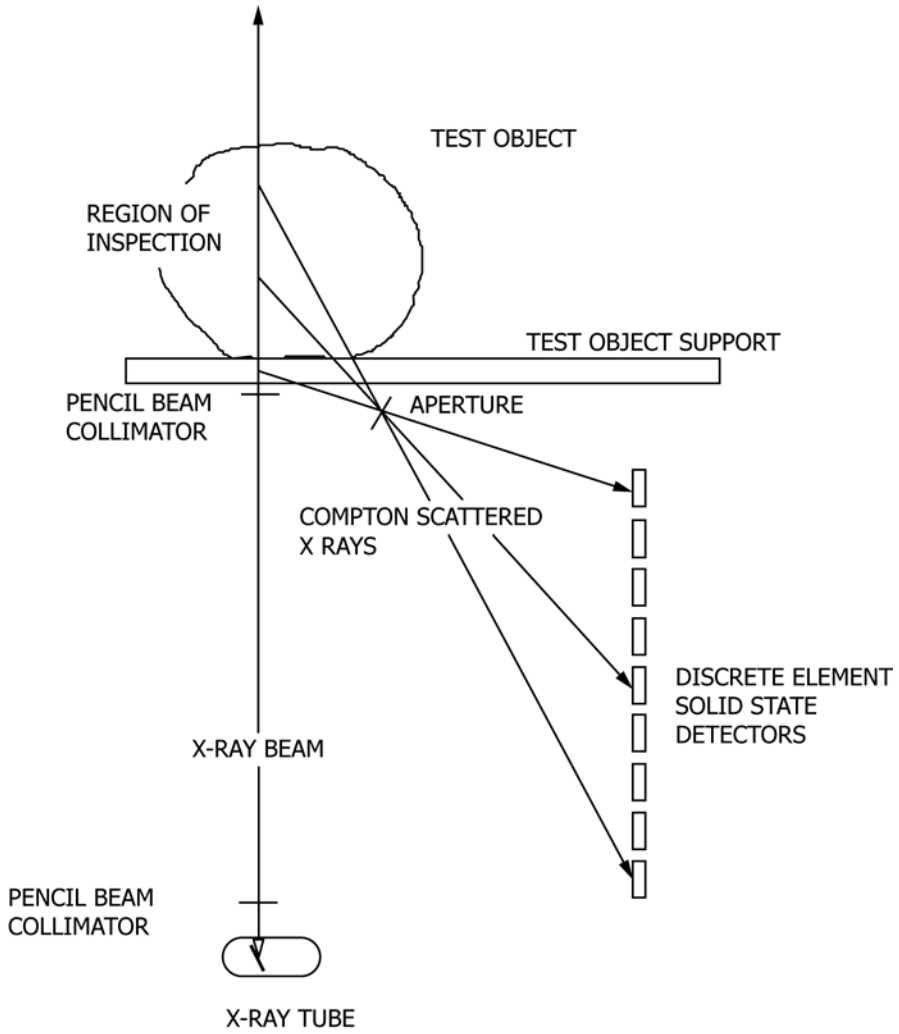

FIG. 9 General Arrangement of X-Ray Source, Detector Array and Examination Object for a Simultaneous Multi-Plane Compton Tomographic Imaging System

therefore receives scatter radiation from incremental depths along the primary X-ray beam to provide simultaneous scatter information lying in nine tomographic slice thicknesses. Moving the examination object or radiation source and detector in an *X* - *Y* raster scan allows all nine slice plane images to be formed simultaneously from individual data points. One technique is to use a flying spot X ray, or scanning pencil beam, in conjunction with a linear array detector to generate complete lines of image data.

8.5 *Data Processing*—Data processing may be utilized to enhance the CST image quality. Because the CST image is a digital image formed in a computer environment, many forms of data processing are possible. One form of raw data processing that is very desirable corrects for decreasing image brightness as the path lengths for the scattered X rays increase as illustrated in Fig. 10. In a homogenous material, it is desirable that the CST image for all tomographic planes have uniform brightness. This brightness non-uniformity may be compensated automatically by subtracting a compensating brightness mask during the initialization of the CST system. These corrections are also referred to as brightness and contrast normalization. Pulse amplitude discrimination, pulse shaping and other techniques commonly employed in photon counting instrumentation may also be utilized with good success. Once the tomographic images are generated, they may be processed by conventional image processing techniques to enhance certain features. For example, a high-pass filter may be utilized to enhance edges. Contrast manipulation may be used to increase image contrast or shift brightness values as may be desired.

8.5.1 Fig. 11 illustrates how a set of slice images may be converted to another set of slice images at a different angle with respect to the original images. This may be desirable when the feature of interest is not accommodated by the initial slice plane orientation. Re-generating the slice images also allows the examination object to be examined from any angle - even tumbled in space to provide an enhanced 3-D effect.

8.6 *Image Data Storage System*—CST images are digital and may therefore be archived on magnetic or optical media without loss of fidelity. Refer to Guide E1453 for information

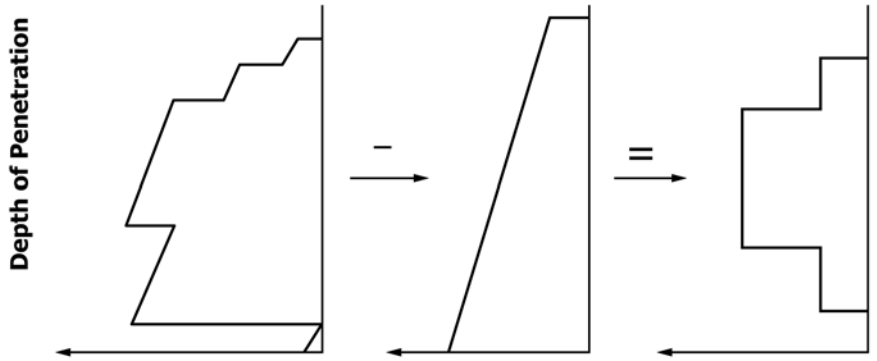

FIG. 10 CST Brightness Data Bias Caused by Differing Tomographic Plane-to-Detector Path Lengths

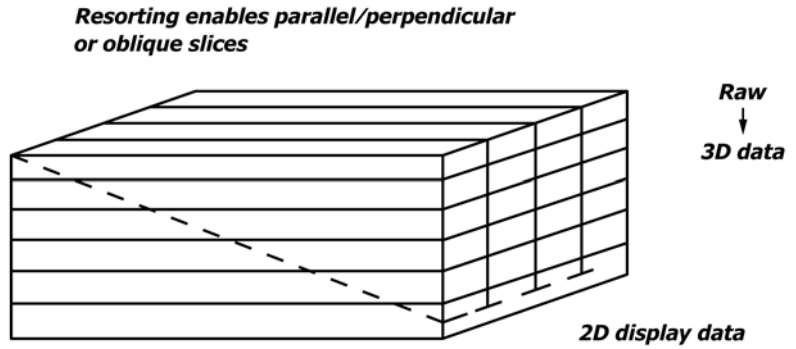

FIG. 11 Tomographic Slice Images May be Generated at Any Angle With Respect to the Original Slice Images

on storage of magnetic media. Guide E1475 contains information on the standardization of data fields containing radiologic examination data.

8.7 *Operator Interface*—The CST system operator interface is similar to other radiologic imaging system interfaces. Typically, the collection and processing of CST data is automated with the operator required only to set up the scan parameters and initiate the process. Tomographic images are presented on a video screen for operator interpretation. Interpretation automatically by computer may be possible for some applications.

9. Procedure

9.1 *Examination Object Requirements*—CST examination has been successfully employed on a wide range of parent materials. These include electronics, plastics, aerospace composite materials, rubber, rocket propellant, aluminum and steel. The best candidates will be lower density materials having a propensity to produce scatter radiation. The technique works well on composites and assemblies where scatter characteristics change abruptly. The detection of corrosion in aluminum aircraft assemblies has been successfully demonstrated. As with all nondestructive testing techniques, a trial on examination objects containing known internal conditions is the best way to determine the suitability of the technique.

9.2 *Equipment Capabilities*—CST equipment tends to be specialized with some systems custom designed for specialized applications. For example, standard CST equipment is available which is powered by 160 keV constant potential industrial X-ray generator. Such equipment can offer the capability of simultaneously producing twenty-two slice plane images. Typical scan depths of up to 50 mm with maximum resolution of 0.4 by 0.4 by 0.4 mm is available. Scan area is 50 by 100 mm. Scan times range from approximately 1 to 6 min depending upon the examination object material and desired image quality.

9.3 *Set-Up*—A proper set-up is critical to the success of CST tomographic imaging. The mechanical set-up must be stable with no relative motion between the radiation source, detector and examination object. The examination volume must be carefully aligned with the examination object as to *X-Y* position and depth. The examination result can be no better than the quality of the mechanical set-up. One of the great advantages of CST is that the set-up is non-contacting and made entirely on one side of the examination object. If an area larger than the scan area is to be examined, it will be necessary to re-position the CST scanner. Re-positioning will require an accurate scan plan lay- out to ensure that no important examination object areas are missed.

9.4 *Radiation Safety*—Radiation shielding is a very important consideration. The radiation energies and intensities associated with the primary radiation beam pose a serious health hazard. The examination object and CST scanner must be suitably radiation shielded in accordance with good radiation safety practices and in accordance with local, state and federal radiation safety requirements. In general, the CST technique is much less difficult to shield than a transmission beam imaging system of similar primary radiation beam energy and intensity. This is due to the fact that the primary radiation beam is highly collimated and closely coupled to the examination object. In

some applications involving thick examination objects, the examination object itself may provide a substantial amount of radiation shielding.

9.5 *Image Quality*—As with all radiologic imaging techniques, image quality is a prime consideration. Unfortunately, most transmission X-ray image quality indicators, such as Test Method E747 or Practice E1025 IQIs, are not useful for CST. Therefore, the user will have to be resourceful in developing phantoms or calibration blocks which accurately represent the examination object's internal conditions. The best calibration block is often an actual examination object whose internal condition has been physically documented by sectioning and re-assembling or by other means. Such a device(s) should be the basis for determining initial image quality and periodically monitoring image quality. This device is known as a Representative Quality Indicator (RQI).

9.6 *Recording of CST Examination Results*—Data storage in a digital format (that is, magnetic or optical media) should be considered for archival quality storage. Guide E1475 contains valuable information on standardized recording data fields for digital radiologic examination data. Image data may be analyzed on the computer display monitor or printed on a digital printer.

10. Interpretation of Results

10.1 This guide does not provide guidance on the interpretation of examination results, that is a matter of agreement between the provider and user of radiologic examination results. This guide attempts to familiarize the reader with the basic theory and practice of CST. As with all radiologic examination techniques, the obtained results depend upon many interrelated factors. Prospective users will be well advised to spend time in an applications laboratory setting before attempting the application of CST in a production setting. The results may be expected to be a function of the specific application. Proper interpretation of CST results depend upon a good understanding of the advantages and disadvantages of CST, the details of the examination object's material and internal structure and the applicable accept/reject criteria.

11. Precision and Bias

11.1 CST is capable of providing both qualitative and quantitative information about an examination object. Qualitative information includes examination object internal features and shapes lying within a known slice. Quantitative information includes three-dimensional information about the location and dimension of internal features. As with all indirect measurement systems, the precision and bias of CST is directly related to the accuracy with which the equipment is calibrated and how closely the measurement technique replicates the calibration technique. Faulty interpretation of the examination results can lead to incorrect qualitative and quantitative measurements even though the equipment is properly calibrated.

11.2 Because of the sources of error listed in the previous section and other potential errors, this guide makes no statement as to the precision and bias of CST.

12. Keywords

12.1 back-scatter; Compton scatter tomography; computed tomography; CST; radiologic; radioscopic; slice image; tomography

APPENDIX

(Nonmandatory Information)

X1. ADDITIONAL PUBLICATIONS

Gray, R. R., et al., "The Measurement of Local Void Fraction With Side-Scatter Gamma Technique," *Proceedings 26th Int. Instr. Symp.*, 1980.

Towe, B.C. and Jacobs, A.M., "X-Ray Back Scatter Imaging," *IEEE Trans. BME 28*, 1981.

Grayer, A. et al., "In-Situ Measurements in Aqueous Solutions by the Gamma Ray Back-Scattering Method," *Nucl. Instr. and Methods 192*, 1982.

Strokes, J.A. et al., "Some New Applications of Collimated Photon Scattering for Non-Destructive Testing Examinations," *Nucl. Instr. and Methods 193*, 1982.

Szepessy, B., "Gamma Reflection Densitometer for the Qualification of Concrete Shieldings," *Periodica Polytechnica 26*, 1982.

Strecker, H., "Scatter Imaging of Aluminum Castings Using an X-Ray Fan Beam and a Pinhole Camera," *Mat. Eval. 40*, 1982.

Harding, G. et al., "X-ray Imaging with Compton Scatter Radiation" *Philips Tech. Rev. 41*, 1983-1984.

Holt, R.S., "Compton Imaging, *Endeavour*, New Series 9, 1985.

Harding, G. and Tischler, R., "Dual Energy Compton Scatter Tomography," *Phys. Med. Biol. 31*, 1986.

The subject is described in standard texts on nuclear physics, such as, Glen Knoll: *Radiation Detection and Measurement*, 3rd Edition, Wiley.

Shedlock, D. et.al. "Optimization of an Rsd X-Ray Backscatter System For Detecting Defects in the Space Shuttle External Tank Thermal Foam Insulation," *Proc. SPIE 5923, Penetrating Radiation Systems and Applications VII*, 59230S, 17 Sept. 2005.

Kolkoori, S., Wrobel, N. Osterloh, K, Zscherpel, U., Ewert, U., "Novel X-Ray Backscatter Technique for Detection of Dangerous Materials: Application to Aviation and Port Security, *Journal of Instrumentation*, Vol. 8, 2013, pp. 1–18.

Abdul-Majid, S., Balamesh, A. "Single Side Imaging of Corrosion Under Insulation Using Single Photon Gamma Backscattering," *Research in Nondestructive Evaluation,* Vol. 25, 2014, pp. 172–85.

Gal, O., Gmar, M. Ivanov, O. et. al., "Development Of A Portable Gamma Camera With Coded Aperture," *Nuclear Instruments and Methods in Physics Research A*, Vol. 563, 2006, pp. 233–37.